Effect of antireflection coating on the crystallization of amorphous silicon films by flash lamp annealing

Yuki Sonoda and Keisuke Ohdaira*

Japan Advanced Institute of Science and Technology, Nomi, Ishikawa 923-1292, Japan

*E-mail: ohdaira@jaist.ac.jp

We succeed in decreasing the fluence of a flash lamp pulse required for the crystallization of electron-beam (EB)-evaporated amorphous silicon (a-Si) films using silicon nitride (SiN_x) antireflection films. The antireflection effect of SiN_x is confirmed not only when SiN_x is placed on the surface of a-Si or flash lamp annealing (FLA) is performed from the film side, but also when SiN_x is inserted between glass and a-Si and a flash pulse is supplied from the glass side. We also quantitatively confirm, by calculating flash lamp pulse energies actually reaching a-Si films using reflectance spectra, that the reduction in the fluence of a flash lamp pulse for the crystallization of a-Si films is due to the antireflection effect of SiN_x.

1. Introduction

In recent years, solar power generation has been expected as a solution to environmental problems and the high power demand. Although current solar cells are mainly wafer-based Si solar cells, their fabrication is not cost-effective since a lot of energy and processes are required for the fabrication of Si wafers. Research on polycrystalline Si (poly-Si) thin-film solar cells has thus been conducted to decrease manufacturing cost.[1-9] Poly-Si films can be formed by crystallizing amorphous Si (a-Si) films by rapid heat treatment on inexpensive substrates with a high productivity. Flash lamp annealing (FLA), i.e., millisecond-order discharge from Xe lamps, is one of the methods applicable to such a rapid heat treatment.[10–15] We have thus far investigated FLA as a method of crystallizing micrometer-order-thick a-Si films.[16–30] In particular, the utilization of electron-beam (EB)-evaporated a-Si films results in the formation of poly-Si films consisting of several tens of micrometer-long grains owing to the occurrence of liquid-phase explosive crystallization during FLA.[26–30] Although this feature is favorable for the application of flash-lamp-crystallized (FLC) poly-Si to solar cells, EB-evaporated a-Si films need a higher fluence for crystallization than a-Si films prepared by other methods.[26–30] The fluence of a flash pulse may be reduced if the loss of a flash lamp pulse light is minimized by suppressing optical reflection.

In this study, we have attempted to utilize silicon nitride (SiN_x) films to reduce the fluence of flash lamp pulse light. The effect of the addition of SiN_x antireflection films is quantitatively confirmed by estimating the energy actually reaching a-Si films using the optical reflectance spectra of a-Si structures. The SiN_x films can be placed not only on the precursor a-Si films but also between a-Si and glass if a flash lamp pulse is irradiated from the glass side. We have not attempted the irradiation of pulse light from the glass side. We

thus also investigate the effects of the sample structure —presence or absence of SiN_x— and the direction of flash pulse irradiation —from the glass side or film side— on the characteristics of FLC poly-Si films.

2. Experimental methods

We used EB-evaporated a-Si structures, as schematically shown in Fig. 1. The a-Si films consisted of a 35-nm-thick n^+-a-Si layer deposited by plasma-enhanced chemical vapor deposition (PECVD), a 2-μm-thick p-type EB-evaporated a-Si film, and a 100-nm-thick EB-evaporated p^+-a-Si layer. Some of the samples had PECVD SiN_x antireflection films with a thickness range of 70–80 nm, as shown in Fig. 1(a). Note that the PECVD SiN_x films were formed without using NH_3, and thus, were expected to contain only a small amount of hydrogen. We also prepared samples with an 85-nm-thick SiN_x film deposited by catalytic chemical vapor deposition (Cat-CVD) on a-Si stacks, as shown in Fig. 1(d). The thickness of the SiN_x films was determined for application to antireflection films in solar cells. Since flash lamp light has a similar spectrum to sunlight[29], the SiN_x films can also have an antireflection effect for flash lamp pulse light. We measured the optical reflectance spectra of these a-Si structures to estimate the energies actually reaching a-Si films. We performed FLA on these a-Si structures. Pulse light was supplied from the glass side for the glass/SiN_x/a-Si and glass/a-Si structures [Figs. 1(a) and 1(b)] and from the a-Si side for the a-Si/glass and SiN_x/a-Si/glass structures [Figs. 1(c) and 1(d)]. FLA was performed using pulse light at fluences of 7–19 J/cm^2 with a duration of 7 ms in Ar atmosphere with preheating of the samples at 500 °C. Only one shot of flash lamp irradiation was performed on each sample. We evaluated the crystallization of the Si films by Raman spectroscopy

using a 632.8 nm line of a He-Ne laser. In addition, we conducted electron spin resonance (ESR) measurements to calculate the defect density of the FLC poly-Si films. The FLC poly-Si films were not intrinsic but doped, and their defect density estimated by ESR might have been underestimated. The doping concentrations of the FLC poly-Si films were, however, identical for the four structures, and their defect densities can be utilized for relative comparison. Although Si dangling bonds are also contained in SiN_x as well as in poly-Si, we can safely neglect the contribution of dangling bonds in SiN_x to the ESR signal since the thickness of poly-Si is much larger than that of SiN_x. We also performed electron backscatter diffraction (EBSD) measurement of the FLC poly-Si films to observe the size and shape of crystal grains.

3. Results and discussion

Figure 2 shows the Raman spectra of the Si films after FLA with a fluence of 12.42 J/cm^2 for the glass/SiN_x/a-Si and glass/a-Si structures. The sample with SiN_x shows a spectrum with a sharp peak from the crystalline Si (c-Si) phase at approximately 520 cm^{-1}, while the sample without SiN_x shows only a broad peak at approximately 480 cm^{-1} originating from the a-Si phase. This demonstrates that the antireflection effect of the additional SiN_x film contributes to the reduction in the fluence of the flash lamp pulse needed for the crystallization of EB-evaporated a-Si films. Note that the c-Si peak of the Raman spectrum for the glass/SiN_x/a-Si structure has a peak at approximately 517 cm^{-1} and a full width at half maximum (FWHM) of ~4.9 cm^{-1}, which are similar to those reported previously.[26–30] These indicate that the FLC poly-Si films formed have a strong tensile stress and consist of relatively large grains.

We also attempted the crystallization of the a-Si/glass and SiN_x/a-Si/glass structures by the irradiation of a flash lamp pulse from the film side, whose Raman spectra are not shown here. The samples with SiN_x are fully crystallized at a fluence of 14.42 J/cm^2, while the sample without SiN_x requires the irradiation of a flash lamp pulse with a fluence of 17.82 J/cm^2. It is thus concluded that the crystallization of an entire a-Si film with a lower energy can be realized using SiN_x films in the cases of both glass- and film-side irradiations.

To quantitatively evaluate the antireflection effect of the SiN_x films, we measured the reflectance of the glass/SiN_x/a-Si, glass/a-Si, a-Si/glass, and SiN_x/a-Si/glass structures, from which we calculated the incident energies of a flash lamp pulse actually reaching a-Si films. Figure 3 shows the optical reflectance spectra of the a-Si samples before crystallization. One can see the lower reflectance for the glass/SiN_x/a-Si and SiN_x/a-Si/glass structures than for the glass/a-Si and a-Si/glass structures. This indicates that the usage of SiN_x antireflection films leads to effective reduction in the optical reflectance. By using the flash pulse fluence at each wavelength $I(\lambda)$, which we reported previously[29], and the optical reflectance $R(\lambda)$ obtained experimentally, the total energy actually reaching a-Si is expressed as

$$\int[1-R(\lambda)]I(\lambda)\mathrm{d}\lambda. \quad (1)$$

We considered only a wavelength range from 300 to 800 nm for this calculation. This is because a-Si films effectively absorb photons only in this wavelength region. Note that the energies calculated using Eq. (1) include the total energy reaching the a-Si films and do not exclude transmitted light.

Table 1 shows the measured the energies required for the crystallization of a-Si films and the calculated energies reaching the a-Si for the glass/SiN_x/a-Si, glass/a-Si, a-Si/glass, and SiN_x/a-Si/glass structures. The measured fluence needed for the crystallization of a-Si films varies widely, depending on the sample structure. On the other hand, the calculated

energies actually reaching a-Si are almost the same, independent of the sample structure. According to this result, we can conclude that the reduction in the fluence of a flash lamp pulse is due to the antireflection effect of SiN_x films.

The addition of SiN_x and the use of different irradiation directions of a flash lamp pulse might lead to the formation of FLC poly-Si films with different properties. We thus evaluated the quality of FLC poly-Si films by Raman spectroscopy, and ESR and EBSD measurements. Figure 4 shows the Raman spectra of Si films after FLA for the glass/SiN_x/a-Si, glass/a-Si, a-Si/glass, and SiN_x/a-Si/glass structures. The actual fluences reaching a-Si for all the samples are approximately 9.5 J/cm^2. All the Raman spectra show c-Si peaks at ~517 cm^{-1} with an FWHM of ~4.5 cm^{-1}. These show that the FLC poly-Si films formed have similar grain sizes and stresses. The large tensile stress results in the formation of cracks in the poly-Si films, as we reported previously;[28] similar cracks are observed in the four structures.

Table II shows the defect densities of the FLC poly-Si films formed from the glass/SiN_x/a-Si, glass/a-Si, a-Si/glass, and SiN_x/a-Si/glass structures. The defect densities of the FLC poly-Si films are on the order of 10^{17} cm^{-3}, independent of the sample structure. Note that the defect densities of the samples with Cat-CVD SiN_x are slightly lower than the samples without Cat-CVD SiN_x. This might be due to the effect of surface passivation by SiN_x and/or the passivation of grain boundaries in the poly-Si films by hydrogen atoms supplied from SiN_x.

Figure 5 shows the EBSD normal direction (ND) color maps of the FLC poly-Si films formed from EB-evaporated a-Si films for the structures shown in Figs. 1(a)–1(c). The EBSD map of the FLC poly-Si film with the structure shown in Fig. 1(d) could not be measured owing to the existence of a SiN_x film on the surface side. All the FLC poly-Si films measured consisted of elongated grains with a length of at least several tens of μm. This

feature probably originates from the occurrence of liquid-phase explosive crystallization during FLA. From these experimental results, we can conclude that the existence of SiN_x films and the irradiation direction of a flash lamp pulse do not significantly affect the quality of poly-Si films. The effective reduction in the fluence of a flash lamp pulse needed for the crystallization of EB-evaporated a-Si films using SiN_x films will contribute to energy saving in the production of FLC poly-Si films.

4. Conclusions

The fluence of a flash lamp pulse for the crystallization of EB-evaporated precursor a-Si films can be effectively reduced using antireflection SiN_x films. We have also quantitatively demonstrated that the actual fluence of the flash lamp pulse reaching the a-Si films needed for crystallization is independent of the sample structure, and that the antireflection effect of SiN_x films is the reason for the reduction in the fluence required for the crystallization. The qualities of poly-Si films are also independent of the irradiation direction of flash lamp light and of the presence or absence of SiN_x films.

Acknowledgments

The authors would like to thank Dr. Sergey Varlamov of University of New South Wales for the preparation of the EB-evaporated a-Si films and Professor Noritaka Usami and Dr. Sergii Tutashkonko of Nagoya University for the EBSD measurement.

References

1) M. A. Green, Sol. Energy **74**, 181 (2003).
2) W. Fuhs, S. Gall, B. Rau, M. Schmidt, and J. Schneider, Sol. Energy **77**, 961 (2004).
3) M. Spitzer, J. Schewchun, E. S. Vera, and J. J. lofersky, Proc. 14th IEEE Photovoltaic Specialists Conf., 1980, p. 375.
4) A. A. D. T. Adikaari, N. K. Mudugamuwa, and S. R. P. Silva, Sol. Energy Mater. Sol. Cells **92**, 634 (2008).
5) J. K. Saha, K. Haruta, M. Yeo, T. Koabayshi, and H. Shirai, Sol. Energy Mater. Sol. Cells **93**, 1154 (2009).
6) T. Matsuyama, M. Tanaka, S. Tsuda, S. Nakano, and Y. Kuwano, Jpn. J. Appl. Phys. **32**, 3720 (1993).
7) M. J. Keevers, T. L. Young, U. Schubert, and M. A. Green, Proc. 22nd European Photovoltaic Solar Energy Conf., 2007, p. 1783.
8) I. Gordon, L. Carnel, D. Van Gestel, G. Beaucarne, J. Poortmans, L. Pinckney, and A. Mayolet, Proc. 22nd European Photovoltaic Solar Energy Conf., 2007, p. 1993.
9) S. Arimoto, H. Morikawa, M. Deguchi, Y. Kawama, Y. Matsuno, T. Ishihara, H. Kumabe, and T. Murotani, Proc. 24th IEEE Photovoltaic Specialists Conf., 1994, p. 1311.
10) B. Pétz, L. Dobos, D. Panknin, W. Skorupa, C. Lioutas, and N. Vouroutzis, Appl. Surf. Sci. **242**, 185 (2005).
11) M. Smith, R. McMahon, M. Voelskow, D. Panknin and W. Skorupa, J. Cryst. Growth **285**, 249 (2005).
12) F. Terai, S. Matsunaka, A. Tauchi, C. Ichikawa, T. Nagatomo, and T. Homma, J.

Electrochem. Soc. **153**, H147 (2006).

13) S. Saxena, D. C. Kim, J. H. Park, and J. Jang, IEEE Electron Device Lett. **31**, 1242 (2010).

14) S. Saxena and J. Jang, IEEE Trans. Electron Devices **58**, 2638 (2011).

15) D. H. Kim, B. K Kim, H. J. Kim, and S. Park, Thin Solid Films **520**, 6581 (2012).

16) K. Ohdaira, Y. Endo, T. Fujiwara, S. Nishizaki, and H. Matsumura, Jpn. J. Appl. Phys. **46**, 7603 (2007).

17) K. Ohdaira, T. Fujiwara, Y. Endo, S. Nishizaki, and H. Matsumura, Jpn. J. Appl. Phys. **47**, 8239 (2008).

18) K. Ohdaira, H. Takemoto, K. Shiba, and H. Matsumura, Appl. Phys. Express **2**, 061201 (2009).

19) K. Ohdaira, T. Fujiwara, Y. Endo, S. Nishizaki, and H. Matsumura, J. Appl. Phys. **106**, 044907 (2009).

20) K. Ohdaira, T. Nishikawa, K. Shiba, H. Takemoto, and H. Matsumura, Phys. Status. Solidi C **7**, 604 (2010).

21) Y. Endo, T. Fujiwara, K. Ohdaira, S. Nishizaki, K. Nishioka, and H. Matsumura, Thin Solid Films **518**, 5003 (2010).

22) K. Ohdaira, J. Vac. Soc. Jpn. **55,** 535 (2012).

23) K. Ohdaira, N. Tomura, S. Ishii, K. Sawada, and H. Matsumura, J. Non-Cryst. Solids **358**, 2154 (2012).

24) K. Ohdaira, Thin Solid Films **575**, 21 (2015).

25) T. Watanabe and K. Ohdaira, Thin Solid Films **595**, 235 (2015).

26) K. Ohdaira, N. Tomura, S. Ishii, and H. Matsumura, Electrochem. Solid-State Lett. **14**, H372 (2011).

27) K. Ohdaira, K. Sawada, N. Usami, S. Varlamov, and H. Matsumura, Jpn. J. Appl. Phys. **51**,

10NB15 (2012).

28) K. Ohdaira and H. Matsumura, J. Cryst. Growth **362**, 149 (2013).

29) K. Ohdaira, Jpn. J. Appl. Phys. **52**, 04CR11 (2013).

30) K. Ohdaira, Can. J. Phys. **92**, 718 (2014).

Figure Captions

Fig. 1. (Color online) Schematics of EB-evaporated a-Si structures: (a) glass/SiN_x/a-Si, (b)glass/a-Si, (c) a-Si/glass, and (d) SiN_x/a-Si/glass. Pulse light was suppled from the glass side for the glass/SiN_x/a-Si and glass/a-Si structures, and from the film side for the a-Si/glass and SiN_x/a-Si/glass structures.

Fig. 2. Raman spectra of Si films after FLA at a fluence of 12.42 J/cm^2 for glass/SiN_x/a-Si and glass/a-Si structures.

Fig. 3. (Color online) Optical reflectance of glass/SiN_x/a-Si, glass/a-Si, a-Si/glass, and SiN_x/a-Si/glass structures.

Fig. 4. Raman spectra of Si films after FLA for glass/SiN_x/a-Si, glass/a-Si, a-Si/glass, and SiN_x/a-Si/glass structures.

Fig. 5. (Color) EBSD ND color maps of FLC poly-Si films formed from (a) glass/SiN_x/a-Si, (b) glass/a-Si, and (c) a-Si/glass structures.

Table I. Experimental fluences of flash lamp pulse and calculated incident energies for glass/SiN_x/a-Si, glass/a-Si, a-Si/glass, and SiN_x/a-Si/glass structures.

	glass/SiN_x/a-Si	glass/a-Si	a-Si/glass	SiN_x/a-Si/glass
Fluence needed for crystallization (J/cm^2)	11.94	14.46	17.38	12.29
Calculated incident energy (J/cm^2)	9.55	9.62	9.47	9.16

Table II. Defect densities (cm^{-3}) of FLC poly-Si films in glass/SiN_x/a-Si, glass/a-Si, a-Si/glass, and SiN_x/a-Si/glass structures.

glass/SiN_x/a-Si	1.2×10^{17}
glass/a-Si	1.3×10^{17}
a-Si/glass	1.7×10^{17}
SiN_x/a-Si/glass	1.2×10^{17}

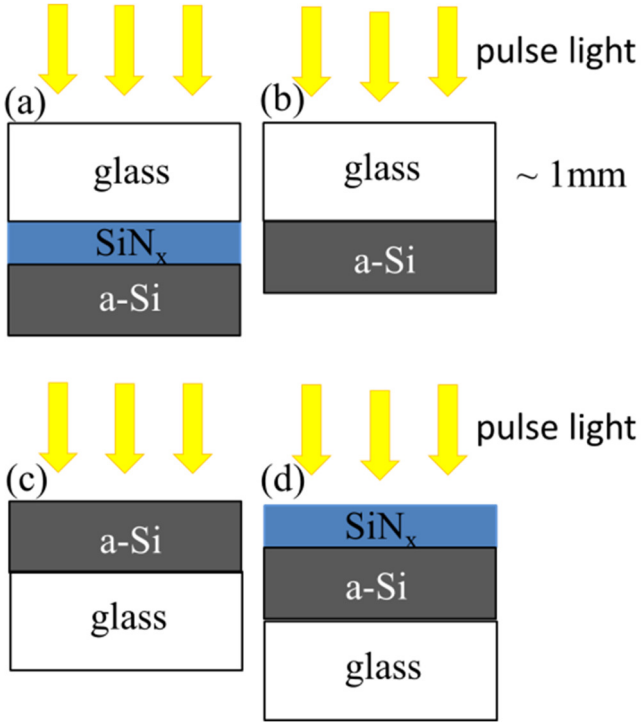

Fig.1. Y. Sonoda *et al*., (Color Online)

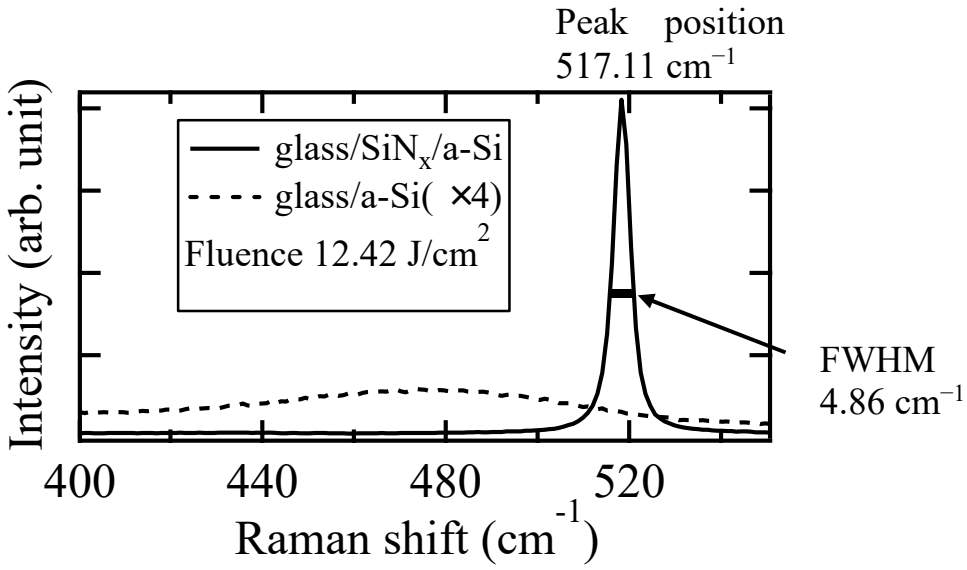

Fig. 2 Y. Sonoda *et al*.,

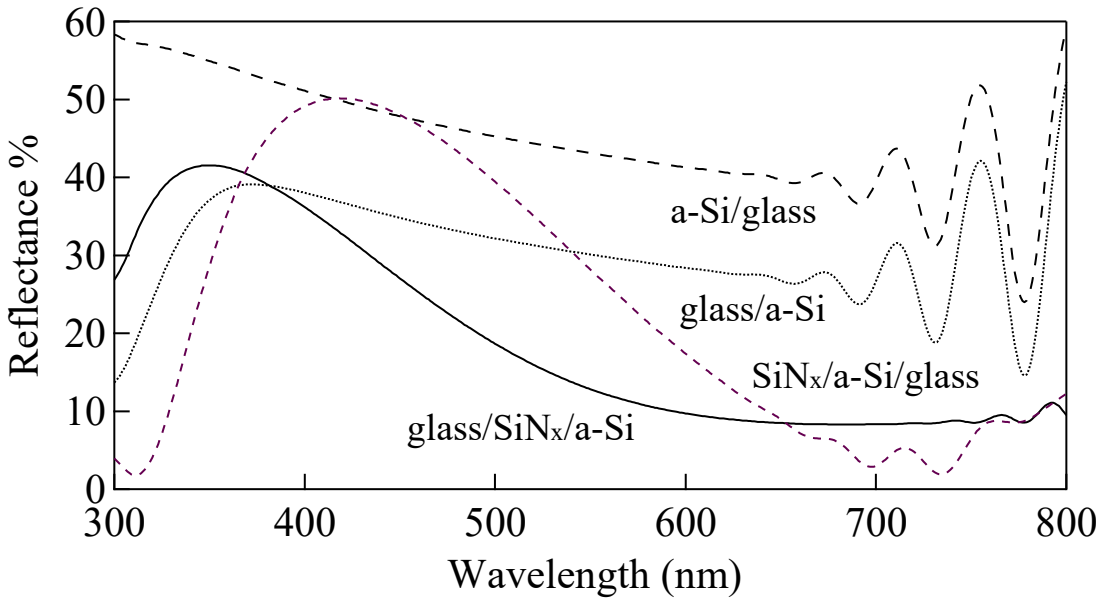

Fig. 3 Y. Sonoda *et al*., (Color Online)

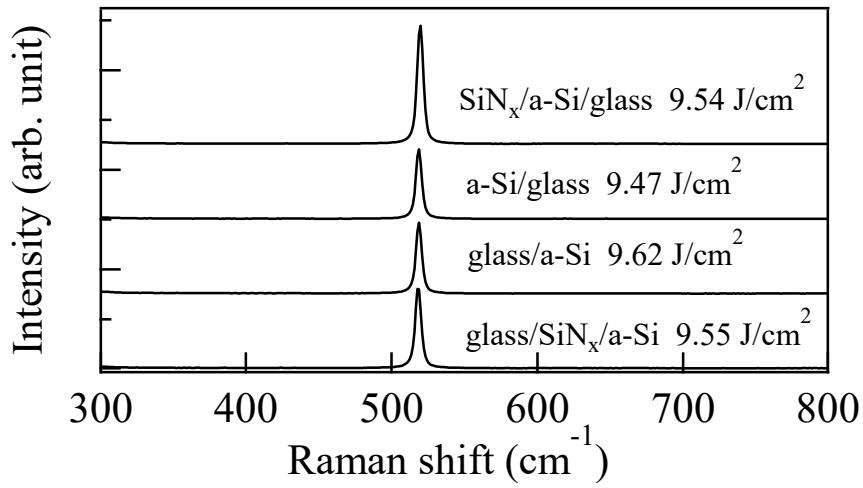

Fig. 4 Y. Sonoda *et al*.,

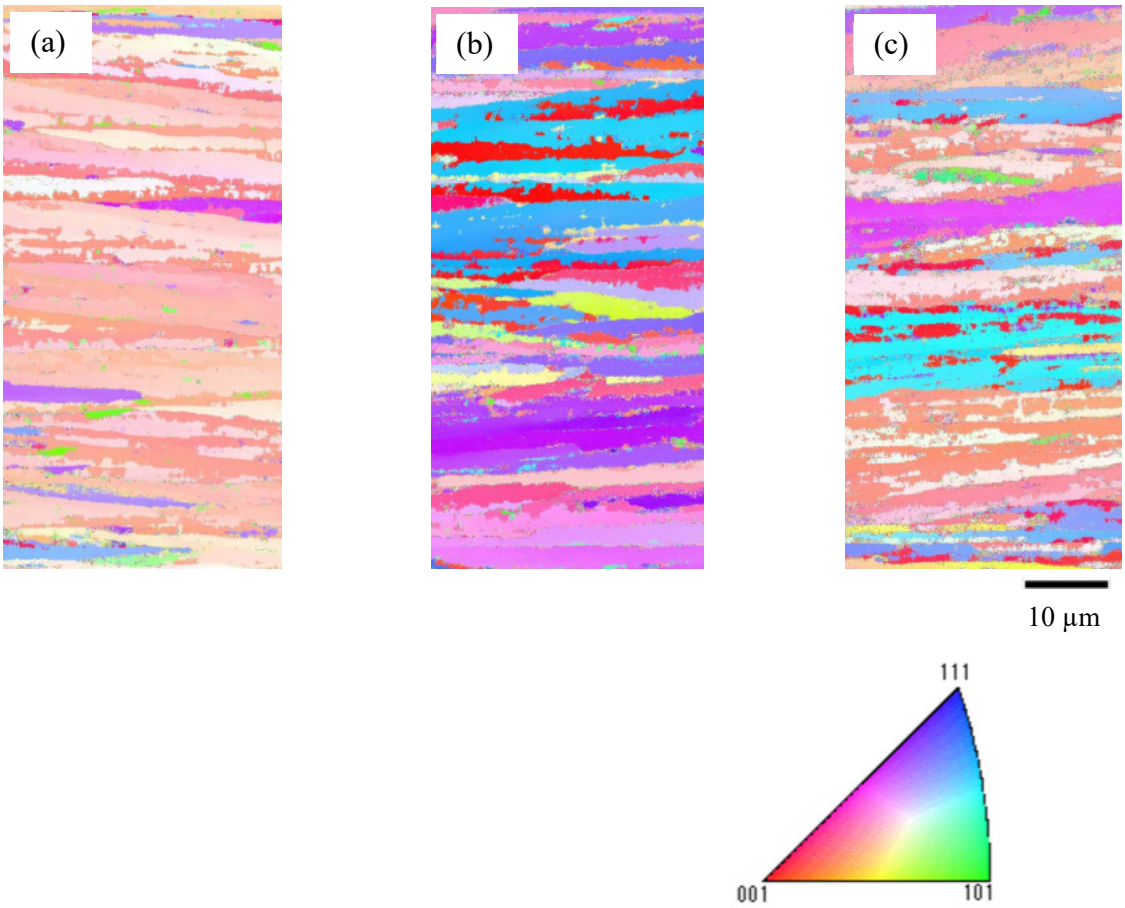

Fig. 5 Y. Sonoda et al., (Color)